PERGAMON

International Journal of Solids and Structures 37 (2000) 5161–5176

INTERNATIONAL JOURNAL OF SOLIDS and STRUCTURES

www.elsevier.com/locate/ijsolstr

On a piezoelectric material containing a permeable elliptical crack

Lu-Ping Chao*, Jin H. Huang

Department of Mechanical Engineering, Feng Chia University, Taichung, 407, Taiwan

Received 12 February 1999; in revised form 16 July 1999

Abstract

This study presents the failure criteria for a permeable crack embedded in an infinite piezoelectric solid, which is separately subjected to a set of uniform electromechanical loads. Based on the equivalent inclusion method, a permeable crack is treated as an elliptical inclusion where its elastic moduli and piezoelectric constants are considered to be zero, while the dielectric constants remain finite. In addition, the interaction between the crack and the applied electromechanical loading is examined by introducing the change of total potential energy function. With this energy function, the energy release rates and the critical loads for fracture are acquired separately in a closed form for a simple tension, in-plane and out-plane shears, and normal electric flux density applied. The closed forms for energy release rate and critical electromechanical loading reveal that they are a function of the aspect ratio of the elliptical crack, the type of the electromechanical loading, and the piezoelectric properties. Moreover, analysis results indicate that the distinct electric fields can retard the dilation of the elliptical crack, particularly for an in-plane electric field incited in perpendicular to the crack faces.

Keywords: Piezoelectric solid; Permeable crack; Equivalent inclusion M; Energy release rate; Aspect ratio; Eshelby tensor; Griffith theory

1. Introduction

Piezoelectric materials have been extensively applied over the last decade to diverse areas such as electromechanical transducers, electronic packaging, solar projector, thermal sensors, underwater acoustic, and medical ultrasonic imaging. This trend may account for why these kinds of materials constitute an important branch of the recently emerging technologies of modern engineering materials. A prominent feature of utilizing piezoelectric materials is the distribution of preexisting defects from

* Corresponding author. Tel.: +886-4451-7250; fax: +886-4451-6545.
E-mail address: lpchao@fcu.edu.tw (L.P. Chao).

0020-7683/00/$ - see front matter
PII: S0020-7683(99)00203-6

which crack propagation can initiate, thereby degrading the strength and stiffness of the materials. Therefore, effectively using piezoelectric materials mandates that the electroelastic response be clearly analyzed from a micromechanics perspective so that the importance of defects (or preexisting cracks) can be thoroughly understood.

Parton (1976) pioneered the analysis of piezoelectric crack problems from a fracture mechanics perspective. That investigation assumed that a slit crack in a piezoelectric solid is traction free, but the electric potential and normal component electric displacement are permeably continuous across the cracked surface. Deeg (1980) proposed the method of distributed dislocations and electric dipoles to resolve an arbitrarily oriented slit crack with impermeable electric fields in a piezoelectric solid. Pak (1990, 1992) employed a complex variable approach to examine the mode III crack problem in a piezoelectric solid and the in-plane electrostatic fields in and around a circular piezoelectric inhomogeneity which was subjected to anti-plane loading. In addition, that investigation derived the stress and electric field intensity factors for different electroelastic loading, which is valid only for a circular inclusion. Kattis et al. (1997, 1998) adopted two-phase potentials methods to study piezoelectric smart composites and worked out for the case the anti-plane deformation. In their study, the piezoelectric composite consisting of two discrete phases of hexagonal piezoelectric crystals is subjected to mechanical and electric loads causing out-of-plane displacements and in-plane electric field. In a related investigation, Dunn (1994) employed the equivalent inclusion method to resolve the closed form of the energy release rate for a permeable elliptical crack in a transversely isotropic piezoelectric solid simultaneously subjected to the antiplane shear stress (mode III) and the in-plane electric loading actuated in perpendicular with crack faces. The so-called permeable crack is that the dielectric constant of crack does not vanish, i.e., electric field can propagate through the crack volume when the small crack volume contains air or some other gas.

However, further efforts must be expended to perform a fracture study of a piezoelectric solid containing a permeable elliptical crack subjected to mechanical loading in mode I, II, and III as well as anti-plane electric field, in-plane electric field incited in parallel or perpendicular with crack faces. Accomplishing such a task would allow us to fully exploit the advantages of piezoelectric materials. Therefore, in this study, we study the closed form of the energy release rate and the critical electromechanical loads for a permeable elliptical crack involved in an infinite piezoelectric solid, which is solely subjected to either one of three kinds of mechanical loading or one of three kinds of electric loading.

The rest of this paper is organized as follows. By modeling the disturbed strain and electric field induced by inclusions, the anisotropic inclusion method (see e.g. Huang and Kuo, 1996; Mura, 1987) is employed to consider the inherently anisotropic coupled behavior of a piezoelectric material. Then, a unified and explicit expression for the coupled electroelastic Eshelby tensors is obtained for the piezoelectric ellipsoidal inclusions in a transversely isotropic medium. Next, the feasibility of using the subsequent tensors in the analysis of a permeable crack is studied. Finally, based on the Griffith (1921) theory, an interaction energy density function is introduced to fully consider the interaction between electromechanical loads and crack extension forces. In light of the results presented herein, the energy release rates and the critical electromechanical loads are explicitly obtained for the fracturing of a piezoelectric cracked solid subjected to different applied loads.

2. Electroelastic Eshelby tensors

The Eshelby tensor (Eshelby, 1957) for isotropic elasticity serves as the foundation for the theory of micromechanics of materials as it is a prerequisite for resolving inclusion problems. This tensor has numerous applications in diverse areas such as fracture mechanics, composite materials, phase

transformation, thermal problems and for materials with defects. Mura (1987) obtained many intriguing results via this tensor. In this section, we establish a similar tensor to resolve piezoelectric inclusion problems.

Following the formulation of Huang and Kuo (1996) we start by considering an infinitely extended piezoelectric solid D containing an ellipsoidal piezoelectric inclusion Ω whose electroelastic moduli L_{iJMn} are the same as the matrix. The shape of reinforcement is considered to be ellipsoid, which can treat composite reinforcement geometrical configurations ranging from the thin flake to continuous fiber reinforcement. Let Z^*_{Mn} be eigenstrain (or stress-free transformation strain) and eigenelectric field (or electric displacement-free transformation electric field) in the inclusion Ω, and zero in the matrix $D-\Omega$. Herein the electroelastic moduli L_{iJMn} and eigenfield Z^*_{Mn} are defined as follows (Huang and Kuo, 1996):

$$L_{iJMn} = \begin{cases} C_{ijmn} & J,\ M \le 3, \\ e_{nij} & J \le 3; M = 4, \\ e_{imn} & J = 4; M \le 3, \\ -k_{in} & J,\ M = 4, \end{cases} \qquad Z^*_{Mn} = \begin{cases} \varepsilon^*_{mn} & M \le 3, \\ -E^*_n & M = 4, \end{cases} \tag{1}$$

where C_{ijmn} denotes the elastic moduli measured at a constant electric field, e_{imn} piezoelectric coefficient measured at a constant strain or electric field, k_{in} dielectric constant measured at a constant strain, ε^*_{mn} eigenstrain, and E^*_n eigenelectric field.

When the eigenstrain and eigenelectric field in the inclusion are uniform, the induced strain ε_{mn}, and the electric field E_n in Ω can be expressed as

$$\varepsilon_{mn} = S_{mnab}\varepsilon^*_{ab} - S_{mn4b}E^*_b, \ -E_n = S_{4n4b}E^*_b - S_{4nab}\varepsilon^*_{ab}, \tag{2}$$

or written in the following unified expression

$$Z_{Mn} = S_{MnAb}Z^*_{Ab} = \begin{cases} S_{mnab}\varepsilon^*_{ab} - S_{mn4b}E^*_b, & M \le 3, \\ S_{4nab}\varepsilon^*_{ab} - S_{4n4b}E^*_b & M = 4, \end{cases} \tag{3}$$

where S_{MnAb} represents a set of four tensors that are referred to as the electroelastic Eshelby tensors analogous to the Eshelby tensor for elasticity. Unless stated otherwise, conventional indicial notation is used where repeated lowercase subscripts are summed over 1 to 3; meanwhile, uppercase subscripts are summed over 1 to 4.

A permeable crack, in which the electric potential and normal component of the electric displacement are continuous across the crack surfaces, are modeled in this work as an elliptical ($a_3 \to \infty$, $a_1/a_2 = a$) inclusion oriented with its generatrix parallel to x_3-axis. In addition, components of the electroelastic Eshelby tensors for elliptical inclusions in a transversely isotropic solid with the x_3-axis normal to the plane of isotropy can be expressed as (Huang and Yu, 1994):

$$S_{1111} = \frac{(2+3a)C_{11} + aC_{12}}{2(1+a)^2 C_{11}}, \quad S_{2222} = \frac{(3a+2a^2)C_{11} + aC_{12}}{2(1+a)^2 C_{11}},$$

$$S_{1122} = \frac{-aC_{11} + (2+a)C_{12}}{2(1+a)^2 C_{11}}, \quad S_{2211} = \frac{-aC_{11} + (a+2a^2)C_{12}}{2(1+a)^2 C_{11}},$$

$$S_{1133} = \frac{C_{13}}{(1+a)C_{11}}, \quad S_{2233} = \frac{aC_{13}}{(1+a)C_{11}},$$

$$S_{1143} = \frac{e_{31}}{(1+a)C_{11}}, \quad S_{2243} = \frac{ae_{31}}{(1+a)C_{11}},$$

$$S_{1212} = S_{1221} = S_{2112} = S_{2121} = \frac{(1+a+a^2)C_{11} - aC_{12}}{2(1+a)^2 C_{11}},$$

$$S_{1313} = S_{1331} = S_{3113} = S_{3131} = \frac{1}{2(1+a)},$$

$$S_{2323} = S_{2332} = S_{3223} = S_{3232} = \frac{a}{2(1+a)},$$

$$S_{4141} = \frac{1}{1+a}, \quad S_{4242} = \frac{a}{1+a}. \tag{4}$$

In arriving at the foregoing equations, the generalized Voigt two-index notation:

$$11\rightarrow 1, \quad 22\rightarrow 2, \quad 33\rightarrow 3, \quad 23\rightarrow 4, \quad 31\rightarrow 5,$$

$$12\rightarrow 6, \quad 41\rightarrow 7, \quad 42\rightarrow 8, \quad 43\rightarrow 9, \tag{5}$$

is adopted to represent the electroelastic moduli L_{iJMn} of the solid.

3. The ellipsoidal inhomogeneity inclusion

Until now, both the matrix and the inclusion have been assumed to have the same electroelastic constants. Next, consider a case involving an ellipsoidal inhomogeneity inclusion, where matrix and inclusion have different electroelastic constants. Moreover, consider a sufficiently large piezoelectric composite D, which contains an ellipsoidal inhomogeneity Ω with the electroelastic moduli L^*_{iJMn}. The surrounding piezoelectric matrix is denoted by $D-\Omega$ and has the electroelastic moduli L_{iJMn}. Let the composite be subjected to a far-field traction and electric displacement $\Sigma^0_{iJ}n_i$, on the boundary with outward unit normal vector n_i, where shorthand notation Σ^0_{iJ} represents

$$\sum_{iJ}^{0} = \begin{cases} \sigma^0_{ij} & J \leq 3, \\ D^0_i & J = 4, \end{cases} \tag{6}$$

with σ^0_{ij} and D^0_i being the applied stress and electric displacement, respectively.

If no inhomogeneity exists, the strain and electric field, Z^0_{Mn}, uniformly distribute over the entire domain. The inhomogeneity provides a disturbance in local fields of both the matrix and inhomogeneity. Let Σ^m_{iJ} and Σ^Ω_{iJ} denote the local disturbances of the stress and electric displacement in the matrix and inhomogeneity, respectively. Hereafter the superscripts 'm' and 'Ω' denote quantities in the matrix and the inhomogeneity respectively. Then, the stress and electric displacement in the inhomogeneity can be expressed as

$$\sum_{iJ}^{0} + \sum_{iJ}^{\Omega} = L^*_{iJMn}(Z^0_{Mn} + Z^m_{Mn} + Z_{Mn}). \tag{7}$$

According to the equivalent inclusion method (Eshelby, 1957), the stress and electric displacement in inhomogeneity can be simulated in an equivalent inclusion with the electroelastic constants of the matrix and a fictitious eigenstrain and eigenelectric field, Z^*_{Mn}. Therefore, Eq. (7) can be written as

$$\sum_{iJ}^{0} + \sum_{iJ}^{\Omega} = L^*_{iJMn}(Z^0_{Mn} + Z^m_{Mn} + Z_{Mn}) = L_{iJMn}(Z^0_{Mn} + Z^m_{Mn} + Z_{Mn} - Z^*_{Mn}). \tag{8}$$

Since the applied load is uniform and the inhomogeneity is ellipsoidal, Z_{Mn} is also uniform in the inhomogeneity (Huang and Yu, 1994), and it can be expressed as a linear function of the fictitious eigenfields Z^*_{Mn}, i.e.,

$$Z_{Mn} = S_{MnAb}Z^*_{Mn}. \tag{9}$$

Therefore, the disturbance of stress and electric displacement in the inhomogeneity can be written by substituting Eq. (9) into Eq. (8) as

$$\sum_{iJ}^{\Omega} = L_{iJMn}Z^m_{Mn} + L_{iJMn}(S_{MnAb} - I_{MnAb})Z^*_{Mn}, \tag{10}$$

where the shorthand notation I_{MnAb} represents the second order and fourth order identity tensors, respectively, i.e.,

$$I_{MnAb} = \begin{cases} (\delta_{ma}\delta_{nb} + \delta_{mb}\delta_{na})/2 & M, A \le 3, \\ \delta_{nb} & M = A = 4, \ . \\ 0 & \text{otherwise} \end{cases} \tag{11}$$

The equivalent eigenstrain and eigenelectric field, Z^*_{Mn}, are resolved by substituting Eq. (9) into the equivalency condition (8). Thus, it can be expressed as follows:

$$h_{iJMn}Z^*_{Mn} = H_{iJnM}\sum_{nM}^{0} \tag{12}$$

where

$$h_{iJMn} = (L^*_{iJAb} - L_{iJAb})S_{AbMn} + L_{iJMn}, \tag{13}$$

$$H_{iJnM} = I_{iJnM} - L^*_{iJAb}L^{-1}_{AbnM}. \tag{14}$$

Since a permeable crack can be understood as the inhomogeneity where its elastic moduli C^*_{ijmn} and piezoelectric constants e^*_{imn} vanish while dielectric constants K^*_{in} remain finite, h_{iJMn} and H_{iJnM} can be simplified in the following matrix forms through the Voigt two-index notation (5):

$$\begin{bmatrix} h_{1111} & h_{1122} & h_{1133} & 0 & 0 & 0 & 0 & 0 & h_{1143} \\ h_{1122} & h_{1111} & h_{1133} & 0 & 0 & 0 & 0 & 0 & h_{2243} \\ h_{3311} & h_{3311} & h_{3333} & 0 & 0 & 0 & 0 & 0 & h_{3343} \\ 0 & 0 & 0 & h_{2323} & 0 & 0 & 0 & h_{2342} & 0 \\ 0 & 0 & 0 & 0 & h_{2323} & 0 & h_{1341} & 0 & 0 \\ 0 & 0 & 0 & 0 & 0 & h_{1122} & 0 & 0 & 0 \\ 0 & 0 & 0 & 0 & h_{1413} & 0 & h_{1441} & 0 & 0 \\ 0 & 0 & 0 & h_{2423} & 0 & 0 & 0 & h_{2442} & 0 \\ h_{3411} & h_{3422} & h_{3433} & 0 & 0 & 0 & 0 & 0 & h_{3443} \end{bmatrix}, \tag{15}$$

$$\begin{bmatrix} H_{1111} & 0 & 0 & 0 & 0 & 0 & 0 & 0 & 0 \\ 0 & H_{2222} & 0 & 0 & 0 & 0 & 0 & 0 & 0 \\ 0 & 0 & H_{3333} & 0 & 0 & 0 & 0 & 0 & 0 \\ 0 & 0 & 0 & H_{2323} & 0 & 0 & 0 & 0 & 0 \\ 0 & 0 & 0 & 0 & H_{1313} & 0 & 0 & 0 & 0 \\ 0 & 0 & 0 & 0 & 0 & H_{1212} & 0 & 0 & 0 \\ 0 & 0 & 0 & 0 & H_{1413} & 0 & H_{1414} & 0 & 0 \\ 0 & 0 & 0 & H_{2423} & 0 & 0 & 0 & H_{2424} & 0 \\ H_{3411} & H_{3422} & H_{3433} & 0 & 0 & 0 & 0 & 0 & H_{3434} \end{bmatrix}. \tag{16}$$

The non-zero entries of h_{iJMn} and H_{iJnM} in the above matrices are tabulated in Appendix A. With h_{iJMn} and H_{iJnM} known, the equivalent eigenfields Z^*_{Mn} in the system of Eqs. (12) can be explicitly solved. Appendix B summarizes those results.

4. Energy release rates

To determine the crack extension force G, a calculation must be made of the change of total potential energy when the crack is extended by the amount Δa_1 shown in Fig. 1. When the far-field surface traction and electric flux density, $\Sigma^0_{iJ}n_i$, is applied on the material's boundary, the change of total

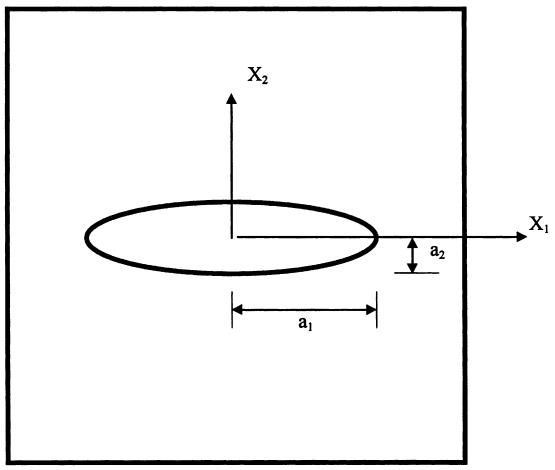

Fig. 1. An elliptical crack in a piezoelectric solid with coordinates denoted the orientation of the crack.

potential energy for the cracked piezoelectric solid is defined as

$$\Delta W = \frac{1}{2}\int_D \left(\sum_{iJ}^{0} + \sum_{iJ}\right)(U^0_{J,\,i} + U_{J,\,i})\mathrm{d}D - \int_{|D|}\left(\sum_{iJ}^{0} n_i\right)(U^0_J + U_J)\mathrm{d}S - \frac{1}{2}\int_D \sum_{iJ}^{0} U^0_{J,\,i}\,\mathrm{d}D - \int_{|D|}\left(\sum_{iJ}^{0} n_i\right)U^0_J\,\mathrm{d}S \tag{17}$$

where $|D|$ denotes the boundary of the composite D.

Since $U_{J,i}$ can be written as $U_{J,i} - Z^*_{Ji} + Z^*_{Ji}$, Z^*_{Ji} is an equivalent eigenstrain and eigenelectric field in Ω when the inhomogeneity is simulated by an equivalent inclusion, we have

$$\sum_{iJ}^{0} U_{J,\,i} = \sum_{iJ}^{0}(U_{J,\,i} - Z^*_{Ji} + Z^*_{Ji}) = L_{iJMn}U^0_{M,\,n}(U_{J,\,i} - Z^*_{Ji} + Z^*_{Ji}) = \sum_{iJ} U^0_{J,\,i} + \sum_{ij}^{0} Z^*_{Ji}. \tag{18}$$

With use of the equations of elastic equilibrium and Gauss' law of electrostatics:

$$\sum_{iJ} n_i = 0 \quad \text{on } |D|, \qquad \sum_{iJ,\,i} = 0 \quad \text{in } D, \tag{19}$$

it can be demonstrated that

$$\int_D \sum_{iJ} U^0_{J,\,i}\,\mathrm{d}D = 0, \tag{20}$$

and

$$\int_D \sum_{iJ} U_{J,\,i}\,\mathrm{d}D = 0. \tag{21}$$

where Gauss' theorem on $|D|$ has been used. Substituting Eqs. (18) and (20) into (17) leads to

$$\Delta W = -\frac{1}{2}\int_\Omega \sum_{iJ}^{0} Z^*_{Ji}\,\mathrm{d}\mathbf{x} = -\frac{1}{2}(2\pi a_1 a_2)\sum_{iJ}^{0} Z^*_{Ji}, \tag{22}$$

where $2\pi a_1 a_2$ denotes the volume per unit thickness of the elliptical crack. The above equation can be easily used to calculate the change of the total potential energy since it involves only the applied electromechanical loads and the equivalent eigenfields.

The energy release rate per unit thickness for an infinitesimal crack extension is defined as

$$G = -\frac{\partial \Delta W}{\partial a_1}. \tag{23}$$

Substituting Z^*_{Mn} listed in Appendix B into Eq. (23) leads to

$$G_{21} = \frac{4(a_1 + a_2)C_{11}\pi\sigma^{0^2}_{21}}{C^{\,2}_{11} - C^{\,2}_{12}} \tag{24}$$

for the in-plane shear stress applied,

$$G_{22} = \frac{(A_0 a_2 A_2 + 4A_0^2 a_1 C_{11} + a_2 A_3 k_{11}^*)\pi\sigma_{22}^{0^2}}{A_0^2 (C_{11} - C_{12})(C_{11} + C_{12})} \tag{25}$$

for the tensile stress applied,

$$G_{23} = \{[a_2^2(2a_1 + a_2)B_0^2 k_{11} + a_2 B_0((a_1 + a_2)(3a_1 + a_2)e_{15}^2 + 2a_1(2a_1 + a_2)C_{44}k_{11}]k_{11}^* + a_1^2 C_{44}[2(a_1 + a_2)e_{15}^2 + (2a_1 + a_2)C_{44}k_{11})k_{11}^{*^2}]\}\pi\sigma_{23}^{0^2}/\{B_0(a_2 B_0 + a_1 C_{44}k_{11}^*)^2\} \tag{26}$$

for the anti-plane shear stress applied,

$$G_{14} = -\frac{a_2 C_{44}[e_{15}^2 + C_{44}(k_{11} - k_{11}^*)][a_1^2 B_0 + a_2(2a_1 + a_2)C_{44}k_{11}^*]\pi D_1^{0^2}}{B_0(a_1 B_0 + a_2 C_{44}k_{11}^*)^2} \tag{27}$$

for in-plane electric loading incited in parallel with crack faces,

$$G_{24} = -\frac{a_2 C_{44}[e_{15}^2 + C_{44}(k_{11} - k_{11}^*)][a_2(2a_1 + a_2)B_0 + a_1^2 C_{44}k_{11}^*]\pi D_2^{0^2}}{B_0(a_2 B_0 + a_1 C_{44}k_{11}^*)^2} \tag{28}$$

for in-plane electric loading incited in perpendicular with crack faces, and

$$G_{34} = -\frac{A_1 a_2(A_0 - A_1 k_{11}^*)\pi D_3^{0^2}}{A_0^2} \tag{29}$$

for electric loading in anti-plane sense applied. The positive coefficients A_0–A_3 and B_0 appearing in preceding equations are defined as

$$A_0 = [2C_{33}e_{31}^2 - 4C_{13}e_{31}e_{33} + (C_{11} + C_{12})e_{33}^2 - 2C_{13}^2 k_{33} + (C_{11} + C_{12})C_{33}k_{33}], \tag{30a}$$

$$A_1 = -2C_{13}^2 + C_{11}C_{33} + C_{12}C_{33}, \tag{30b}$$

$$A_2 = (C_{11} + C_{12})[-2C_{13}e_{31}e_{33} + C_{11}e_{33}^2 - C_{13}^2 k_{33} + C_{33}(e_{31}^2 + C_{11}k_{33})], \tag{30c}$$

$$A_3 = (C_{11} - C_{12})(C_{11} + C_{12})(C_{33}e_{31} - C_{13}e_{33})^2, \tag{30d}$$

$$B_0 = e_{15}^2 + C_{44}k_{11}. \tag{30e}$$

Eqs. (24)–(26) are the closed forms of the energy release rate for an elliptical permeable crack embedded in an infinite piezoelectric solid under distinct types of mechanical loading. Correspondingly, being subjected to different types of electric loading, the closed forms of the release rates for the crack are represented in Eqs. (27)–(29), in which the minus sign physically indicates that the distinct electric fields can retard the crack propagation.

Next, as a numerical example to emphasize the physical dimension of these closed forms for the energy release rate, lead zirconate titante (PTZ-5H) piezoceramic is illustrated herein. Its material properties are represented as follows (Pak, 1992).

$C_{11} = 126$ GPa, $C_{12} = 55$ GPa, $C_{13} = 53$ GPa,

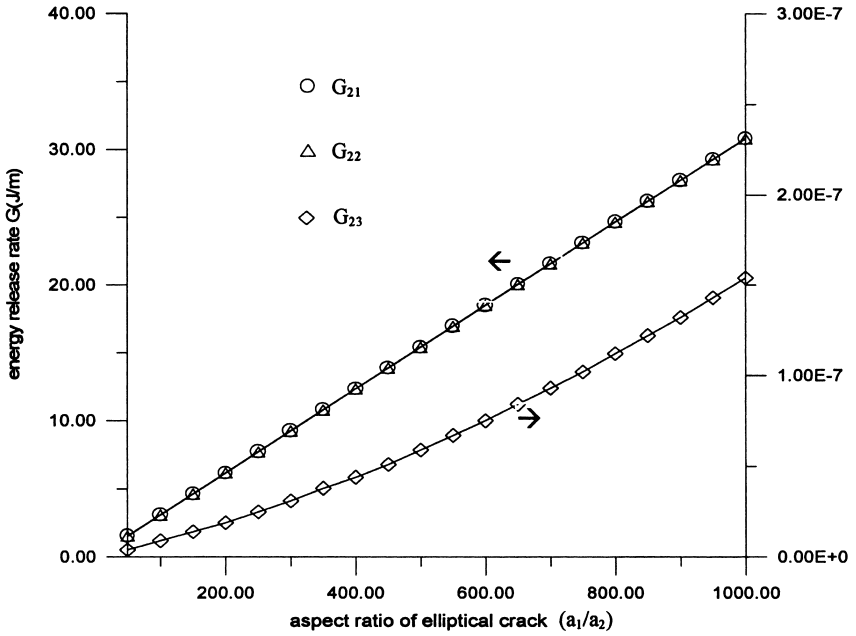

Fig. 2. Energy release rate of PTZ-5H piezoceramic vs aspect ratio of the crack under three kinds of mechanical loading applied.

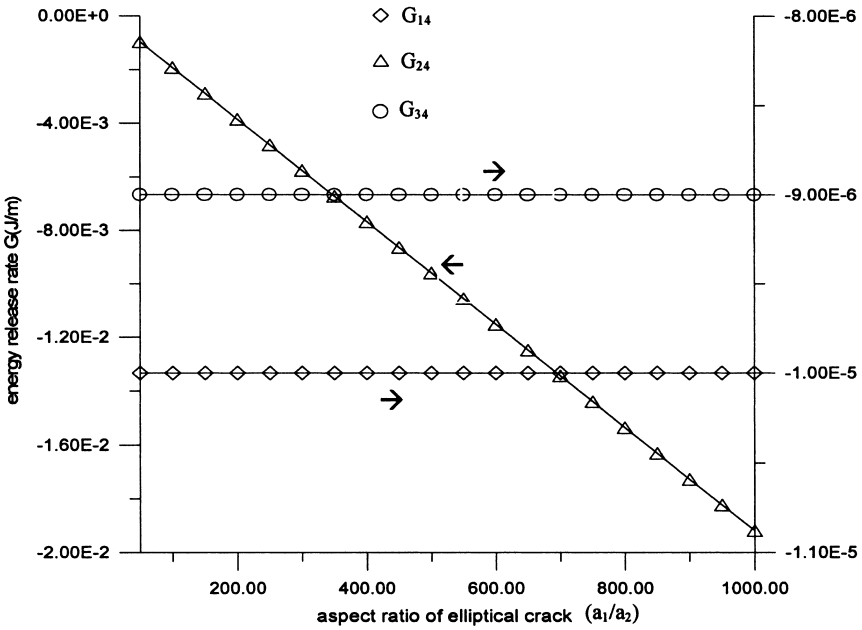

Fig. 3. Energy release rate of PTZ-5H piezoceramic vs aspect ratio of the crack under three types of electric fields incited.

$$C_{33} = 117 \text{ GPa}, \quad C_{44} = 35.3 \text{ GPa},$$

$$e_{31} = -6.5 \text{ C/m}^2, \quad e_{33} = 23.3 \text{ C/m}^2, \quad e_{15} = 17 \text{ C/m}^2,$$

$$k_{11} = 1.51 \times 10^{-8} \text{ C/Vm}, \quad k_{33} = 1.30 \times 10^{-8} \text{ C/Vm},$$

$$k_{11}^* = k_{22}^* = k_{33}^* = 8.85 \times 10^{-12} \text{ C/Vm}. \tag{31}$$

where GPa denotes the giganewtons per square meter, C represents the charge in coulombs, and V is the electric potential in volts. According to the numerical results, Fig. 2 exhibits that the energy release rate linearly increases with respect to the extension of the aspect ratio (a_1/a_2) of the elliptical crack under mechanical loading applied. This coincides with the conventional fracture criterion. Fig. 3 displays the energy release rates versus the aspect ratio of the elliptical crack subjected to three distinct sense of electric loading with the minus values of the energy release rate. This finding suggests that the electric loading can diminish the dilation of the elliptical flaw. According to this Fig. 3, the in-plane electric loading applied in perpendicular with crack faces significantly influences the retarding effect of the dilation of the crack, compared with another two types of electric loading.

5. Critical electromechanical loads

The critical stress and electric displacement for the crack to be distended under distinct mechanical loading or electric field can be determined according to the Griffith fracture criterion (see e.g. Griffith, 1921)

$$\frac{\partial}{\partial a_1}(\Delta W + 2\pi a_1 a_2 \gamma) = 0, \tag{32}$$

where γ denotes the surface energy density of the piezoelectric material. Substituting Z_{Mn}^* tabulated in Eqs. (B1)–(B14) into Eq. (32) leads to

$$\sigma_{21}^c = \sqrt{\frac{a_2(C_{11}^{\,2} - C_{12}^{\,2})\gamma}{2(a_1 + a_2)C_{11}}} \tag{33}$$

for the critical in-plane shear stress,

$$\sigma_{22}^c = \sqrt{\frac{2A_0^2 a_2(C_{11} - C_{12})(C_{11} + C_{12})\gamma}{A_0 a_2 A_2 + 4A_0^2 a_1 C_{11} + a_2 A_3 k_{11}^*}} \tag{34}$$

for the critical tensile stress,

$$\sigma_{23}^c = \{2a_2 B_0(a_2 B_0 + a_1 C_{44} k_{11}^*)^2 \gamma\}^{1/2} / \{a_2^2(2a_1 + a_2)B_0^2 k_{11} + a_2 B_0[(a_1 + a_2)(3a_1 + a_2)e_{15}^2 + 2a_1(2a_1 + a_2)C_{44}k_{11}]k_{11}^* + a_1^2 C_{44}[2(a_1 + a_2)e_{15}^2 + (2a_1 + a_2)C_{44}k_{11}]k_{11}^{*^2}\}^{1/2} \tag{35}$$

for the critical anti-plane shear stress,

$$D_1^c = \sqrt{\frac{-2B_0(a_1B_0 + a_2C_{44}k_{11}^*)^2\gamma}{C_{44}(B_0 - C_{44}k_{11}^*)(a_1^2B_0 + a_2(2a_1 + a_2)C_{44}k_{11}^*)}} \tag{36}$$

for the critical electric displacement in the x_1 direction,

$$D_2^c = \sqrt{\frac{-2B_0(a_2B_0 + a_1C_{44}k_{11}^*)^2\gamma}{C_{44}(B_0 - C_{44}k_{11}^*)(a_2(2a_1 + a_2)B_0 + a_1^2C_{44}k_{11}^*)}} \tag{37}$$

for the critical electric displacement in the x_2 direction, and

$$D_3^c = \sqrt{\frac{-2A_0^2\gamma}{A_1(A_0 - A_1k_{11}^*)}} \tag{38}$$

for the critical electric displacement in the x_3 direction.

Fig. 4 depicts the numerical demonstration with PTZ-5H piezoceramic for the closed forms of the critical stresses in Eqs. (33)–(35), where the critical stresses are monotonously decreased with respect to the extension of aspect ratio of the elliptical crack. The critical anti-plane shear stress in this Fig. 4 has an enormous value correlated with the critical in-plane shear stress and the tensile stress. This finding suggests that the elliptical crack is difficult to be ruptured under the mechanical loading applied in anti-plane shear sense. Eqs. (36)–(38) are the closed forms of the critical electric displacement, in which the value inside the root symbol is always negative. The negative value physically implies that the trade of the crack propagation becomes retarded when electric field loading is applied to the piezoelectric solid.

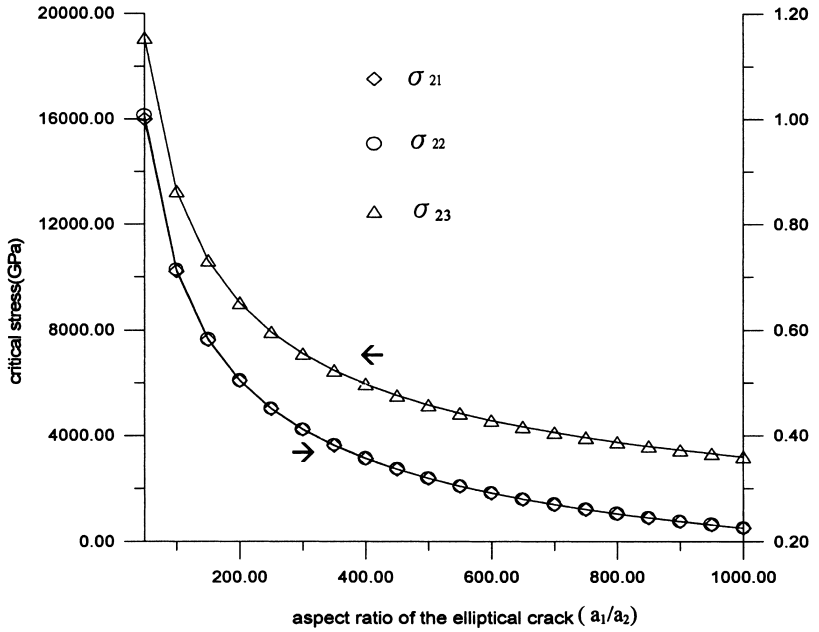

Fig. 4. The variation of critical stress for PTZ-5H piezoceramic with respect to aspect ratio subjected to three kinds of mechanical loading.

6. Conclusions

This study theoretically presents the fracture criterion in a closed form for an infinite piezoelectric solid containing a permeable elliptical flaw separately subjected to three modes of mechanical loading and three forms of electric loading. The energy release rates are introduced herein to quantitatively determine the crack extension force. In addition, the critical mechanical stress and critical electric displacement are employed to forecast the trade of the crack propagation. Moreover, the closed forms for energy release rate and critical electromechanical loading indicate that they are functions of the aspect ratio of the crack, the type of the electromechanical loading, and the piezoelectric properties. Furthermore, explicit results in this study demonstrate that the distinct electric fields can delay the crack propagation. In addition, the in-plane electric field induced perpendicularly with crack faces has a profound influence in terms of retarding the dilation of the elliptical crack. The results obtained herein for a permeable elliptical crack containing in a piezoelectric solid subjected to one of the electromechanical loading can be extended not only to resolve a permeable crack simultaneously subjected to mechanical loading and electrical loading, but also to develop the fracture criterion for a piezoelectric material containing multiple elliptical cracks.

Acknowledgements

The authors wish to thank the National Science Council of the Republic of China for financially supporting this research under contracts Nos NSC 85-2212-E-035-010 and NSC 87-2216-E-035-016.

Appendix A

The non-zero components of h_{iJMn} and H_{iJnM} in Eqs. (15) and (16) respectively, are listed in the following

$$h_{1111} = \frac{a(1+2a)(C_{11}^{\,2} - C_{12}^{\,2})}{2(1+a)^2 C_{11}}, \quad h_{1122} = \frac{a(C_{11}^{\,2} - C_{12}^{\,2})}{2(1+a)^2 C_{11}},$$

$$h_{1133} = \frac{a(C_{11} - C_{12})C_{13}}{(1+a)C_{11}}, \quad h_{1143} = \frac{a(C_{11} - C_{12})e_{31}}{(1+a)C_{11}},$$

$$h_{2222} = \frac{(2+a)(C_{11}^{\,2} - C_{12}^{\,2})}{2(1+a)^2 C_{11}}, \quad h_{2233} = \frac{(C_{11} - C_{12})C_{13}}{(1+a)C_{11}},$$

$$h_{2243} = \frac{(C_{11} - C_{12})e_{31}}{(1+a)C_{11}}, \quad h_{3311} = \frac{a(C_{11} - C_{12})C_{13}}{(1+a)C_{11}},$$

$$h_{3322} = \frac{(C_{11} - C_{12})C_{13}}{(1+a)C_{11}}, \quad h_{3333} = -\frac{C_{13}^{\,2}}{C_{11}} + C_{33},$$

$$h_{3343} = -\frac{C_{13}e_{31}}{C_{11}} + e_{33}, \quad h_{2323} = \frac{C_{44}}{1+a}$$

$$h_{2342} = \frac{e_{15}}{1+a}, \quad h_{1313} = \frac{aC_{44}}{1+a}$$

$$h_{1341} = \frac{ae_{15}}{1+a}, \quad h_{1413} = \frac{ae_{15}}{1+a}$$

$$h_{1441} = \frac{-a(k_{11}+k_{11}^*)}{1+a}, \quad h_{2423} = -\frac{e_{15}}{1+a}$$

$$h_{2442} = \frac{-(k_{11}+ak_{11}^*)}{1+a}, \quad h_{3411} = \frac{a(C_{11}-C_{12})e_{31}}{(1+a)C_{11}}$$

$$h_{3422} = \frac{(C_{11}-C_{12})e_{31}}{(1+a)C_{11}}, \quad h_{3433} = \frac{-C_{13}e_{31}}{C_{11}} + e_{33},$$

$$h_{3443} = \frac{-(e_{31}^2 + C_{11}k_{33})}{C_{11}}$$

$$H_{1111} = H_{2222} = H_{3333} = 1$$

$$H_{1212} = H_{1313} = H_{2323} = \frac{1}{2}$$

$$H_{1413} = H_{2423} = \frac{e_{15}k_{11}^*}{2(e_{15}^2 + C_{44}k_{11})}$$

$$H_{1414} = H_{2424} = 1 - \frac{C_{44}k_{11}^*}{e_{15}^2 + C_{44}k_{11}}$$

$$H_{3411} = H_{3422} = \frac{(C_{33}e_{31}k_{11}^* - C_{13}e_{33}k_{11}^*)}{2C_{33}e_{31}^2 - 4C_{13}e_{31}e_{33} + (C_{11}+C_{12})e_{33}^2 - 2C_{13}^2k_{33} + (C_{11}+C_{12})C_{33}k_{33}}$$

$$H_{3433} = \frac{[2C_{13}e_{31} - (C_{11}+C_{12})e_{33}]k_{11}^*}{4C_{13}e_{31}e_{33} - (C_{12}+C_{12})e_{33}^2 + 2C_{13}^2k_{33} - C_{33}(2e_{31}^2 + (C_{11}+C_{12})k_{33})}$$

$$H_{3434} = 1 - \frac{[2C_{13}^2 - (C_{11}+C_{12})C_{33}]k_{11}^*}{4C_{13}e_{31}e_{33} - (C_{12}+C_{12})e_{33}^2 + 2C_{13}^2k_{33} - C_{33}(2e_{31}^2 + (C_{11}+C_{12})k_{33})}.$$

Appendix B

The equivalent eigen-strain and eigen-electric field obtained from Eq. (12) are given below. For the in-plane shear stress σ_{21}^0 applied in piezoelectric solid:

$$Z^{o}_{21} = \frac{(1+a)^2 C_{11}\sigma^0_{21}}{a(C^{\,2}_{11} - C^{\,2}_{12})}. \tag{B1}$$

For the tensile stress $\sigma^{\,0}_{22}$ applied in piezoelectric:

$$\begin{aligned} Z^{*}_{11} = -\{&[C^{\,3}_{11}(e^2_{33} + C_{33}k_{33})^2 + C_{11}(6C^{\,2}_{33}e^4_{31} - 24C_{13}C_{33}e^3_{31}e_{33} + 24C^{\,2}_{13}e^2_{31}e^2_{33} + 4C_{12}C_{33}e^2_{31}e^2_{33} \\ &- 8C_{12}C_{13}e_{31}e^3_{33} + C^{\,2}_{12}e^4_{33} + 2(2C_{33}(-3C^{\,2}_{13} + C_{12}C_{33})e^2_{31} + 4C_{13}(3C^{\,2}_{13} - C_{12}C_{33})e_{31}e_{33} \\ &+ C_{12}(-2C^{\,2}_{13} + C_{12}C_{33})e^2_{33})k_{33} + (6C^{\,4}_{13} - 4C_{12}C^{\,2}_{13}C_{33} + C^{\,2}_{12}C^{\,2}_{33})k^2_{33}] + C^{\,2}_{11}[(e^2_{33} \\ &+ C_{33}k_{33})(5C_{33}e^2_{31} - 10C_{13}e_{31}e_{33} + 2C_{12}e^2_{33} - 5C^{\,2}_{13}k_{33} + 2C_{12}C_{33}k_{33}) - (C_{33}e_{31} \\ &- C_{13}e_{33})^2 k^*_{11}] + C_{12}[-(2C_{33}e^2_{31} - 4C_{13}e_{31}e_{33} + C_{12}e^2_{33} - 2C^{\,2}_{13}k_{33} + C_{12}C_{33}k_{33})(C_{33}e^2_{31} \\ &- C_{13}(2e_{31}e_{33} + C_{13}k_{33})) + C_{12}(C_{33}e_{31} - C_{13}e_{33})^2 k^*_{11}]\}\sigma^0_{22}/\{(C_{11} - C_{12})(C_{11} + C_{12}) \\ &\times (2C_{33}e^2_{31} - 4C_{13}e_{31}e_{33} + (C_{11} + C_{12})e^2_{33} - 2C^{\,2}_{13}k_{33} + (C_{11} + C_{12})e^2_{33}\} \end{aligned} \tag{B2}$$

$$\begin{aligned} Z^{*}_{22} = \{&[(2C_{33}e^2_{31} - 4C_{13}e_{31}e_{33} + (C_{11} + C_{12})e^2_{33} - 2C^{\,2}_{13}k_{33} + (C_{11} + C_{12})C_{33}k_{33})((1 \\ &+ 2a)C^{\,2}_{11}(e^2_{33} + C_{33}k_{33}) + C_{11}(e_{33}(-2(1+4a)C_{13}e_{31} + (1+2a)C_{12}e_{33}) - (1+4a)C^{\,2}_{13}k_{33} \\ &+ C_{33}(e^2_{31} + 4ae^2_{31} + C_{12}k_{33} + 2aC_{12}k_{33})) + C_{12}(C_{33}e^2_{31} - C_{13}(2e_{31}e_{33} + C_{13}k_{31})))(C_{11} \\ &- C_{12})(C_{11} + C_{12})(C_{33}e_{31} - C_{13}e_{33})^2 k^*_{11}]\sigma^0_{22}\}/\{(C_{11} - C_{12})(C_{11} + C_{12})(2C_{33}e^2_{31} \\ &- 4C_{13}e_{31}e_{33} + (C_{11} + C_{12})e^2_{33} - 2C^{\,2}_{13}k_{33} + (C_{11} + C_{12})C_{33}k_{33})^2\} \end{aligned} \tag{B3}$$

$$\begin{aligned} Z^{*}_{33} = -\{&[(e_{31}e_{33} + C_{13}k_{33})(2C_{33}e^2_{31} - 4C_{13}e_{31}e_{33} + (C_{11} + C_{12})e^2_{33} - 2C^{\,2}_{13}k_{33} + (C_{11} \\ &+ C_{12})C_{33}k_{33})(-2C_{13}e_{31} + (C_{11} + C_{12})e_{33})(-C_{33}e_{31} + C_{13}e_{33})k^*_{11}]\sigma^0_{22}\}/\{2C_{33}e^2_{31} \\ &- 4C_{13}e_{31}e_{33} + (C_{11} + C_{12})e^2_{33} - 2C^{\,2}_{13}k_{33} + (C_{11} + C_{12})C_{33}k_{33}\}^2 \end{aligned} \tag{B4}$$

$$\begin{aligned} Z^{*}_{43} = &[(C_{33}e_{31} - C_{13}e_{33})(-4C_{13}e_{31}e_{33} + (C_{11} + C_{12})e^2_{33} + C_{33}(2e^2_{31} + (C_{11} + C_{12})(k_{33} - k^*_{11})) \\ &- 2C^{\,2}_{13}(k_{33} - k^*_{11})]\sigma^0_{22}/[2C_{33}e^2_{31} - 4C_{13}e_{31}e_{33} + (C_{11} + C_{12})e^2_{33} - 2C^{\,2}_{13}k_{33} + (C_{11} \\ &+ C_{12})C_{33}k_{33}]^2 \end{aligned} \tag{B5}$$

For the anti-plane shear stress $\sigma^{\,0}_{23}$ applied in piezoelectric solid:

$$Z^{*}_{23} = \frac{(1+a)[C_{44}k_{11}(k_{11} + ak^*_{11}) + e^2_{15}(k_{11} + k^*_{11} + ak^*_{11})]\sigma_{23}}{2(e^2_{15} + C_{44}k_{11})(e^2_{15} + C_{44}k_{11} + aC_{44}k^*_{11})} \tag{B6}$$

$$Z^*_{42} = \frac{(1+a)e_{15}[e^2_{15} + C_{44}(k_{11} - k^*_{11})]\sigma_{23}}{(e^2_{15} + C_{44}k_{11})(e^2_{15} + C_{44}k_{11} + aC_{44}k^*_{11})} \tag{B7}$$

For in-plane electric loading D^0_1 incited in parallel with crack faces:

$$Z^*_{13} = \frac{(1+a)e_{15}[e^2_{15} + C_{44}(k_{11} - k^*_{11})]D^0_1}{2(e^2_{15} + C_{44}k_{11})(ae^2_{15} + aC_{44}k_{11} + C_{44}k^*_{11})} \tag{B8}$$

$$Z^*_{41} = -\frac{(1+a)C_{44}(e^2_{15} + C_{44}(k_{11} - k^*_{11}))D^0_1}{(e^2_{15} + C_{44}k_{11})(ae^2_{15} + aC_{44}k_{11} + C_{44}k^*_{11})} \tag{B9}$$

For in-plane electric loading D^0_2 incited in perpendicular with crack faces:

$$Z^*_{23} = \frac{(1+a)e_{15}(e^2_{15} + C_{44}(k_{11} - k^*_{11}))D^0_2}{2(e^2_{15} + C_{44}k_{11})(e^2_{15} + C_{44}k_{11} + aC_{44}k^*_{11})} \tag{B10}$$

$$Z^*_{42} = -\frac{(1+a)C_{44}(e^2_{15} + C_{44}(k_{11} - k^*_{11}))D^0_2}{(e^2_{15} + C_{44}k_{11})(e^2_{15} + C_{44}k_{11} + aC_{44}k^*_{11})} \tag{B11}$$

For anti-plane electric loading D^0_3 applied only:

$$\begin{aligned} Z^*_{11} &= Z^*_{22} \\ &= \{(C_{33}e_{31} - C_{13}e_{33})[-4C_{13}e_{31}e_{33} + (C_{11} + C_{12})e^2_{33}C_{33}(2e^2_{31} + (C_{11} + C_{12})(k_{33} - k^*_{11})) \\ &\quad - 2C^{\,2}_{13}(k_{33} - k^*_{11})]D^0_3\}/\{2C_{33}e^2_{31} - 4C_{13}e_{31}e_{33} + (C_{11} + C_{12})e^2_{33} - 2C^{\,2}_{13}k_{33} + (C_{11} \\ &\quad + C_{12})C_{33}k_{33}\}^2 \end{aligned} \tag{B12}$$

$$\begin{aligned} Z^*_{33} = \{&[2C_{13}e_{31} - (C_{11} + C_{12})e_{33}][4C_{13}e_{31}e_{33} - (C_{11} + C_{12})e^2_{33} - C_{33}(2e^2_{31} + (C_{11} + C_{12})(k_{33} \\ &- k^*_{11})) + 2C^{\,2}_{13}(k_{33} - k^*_{11})]D^0_3\}/\{2C_{33}e^2_{31} - 4C_{13}e_{31}e_{33} + (C_{11} + C_{12})e^2_{33} - 2C^{\,2}_{13}k_{33} \\ &+ (C_{11} + C_{12})C_{33}k_{33}\}^2 \end{aligned} \tag{B13}$$

$$\begin{aligned} Z^*_{43} = -\{&[2C^{\,2}_{13} - (C_{11} + C_{12})C_{33}][4C_{13}e_{31}e_{33} - (C_{11} + C_{12})e^2_{33} - C_{33}(2e^2_{31} + (C_{11} + C_{12})(k_{33} \\ &- k^*_{11})) + 2C^{\,2}_{13}(l_{33} - k^*_{11})]D^0_3\}/\{2C_{33}e^2_{31} - 4C_{13}e_{31}e_{33} + (C_{11} + C_{12})e^2_{33} - 2C^{\,2}_{13}k_{33} + (C_{11} \\ &+ C_{12})C_{33}k_{33}\}^2 \end{aligned} \tag{B14}$$

References

Deeg, W.F., 1980. The analysis of dislocation, cracks and inclusion problems in piezoelectric solids. Ph.D. dissertation, Stanford University.

Dunn, M.L., 1994. The effects of crack face boundary conditions on the fracture mechanics of piezoelectric solids. Engineering Fracture Mechanics 48, 25–39.

Eshelby, J.D., 1957. The determination of the elastic field of an ellipsoidal inclusion, and related problems. Proc. Roy. Soc. A241, 376–396.

Griffith, A.A., 1921. The phenomena of rupture and flow in solid. Trans. Roy. Soc. A221, 163–179.

Huang, J.H., Kuo, W.S., 1996. Micromechanics determination of the effective properties of piezoelectric composites containing spatially oriented shorted fibers. Acta Metal. Mater. 44, 4889–4898.

Huang, J.H., Yu, J.S., 1994. Electroelastic Eshelby's tensors for an ellipsoidal piezoelectric inclusion. Composite Engineering 4, 1169–1182.

Kattis, M.A., Providas, E., Boutalis, Y., Kalamkarov, A.L., 1997. Antiplane deformation of partially bounded elliptical inclusion. Int. J. Theoretical and Applied Fracture Mechanics 27, 43–51.

Kattis, M.A., Providas, E., Kalamkarov, A.L., 1998. Two-phase potentials in the analysis of smart composites having piezoelectrical components. Composites Parts B: Engineering Journal 29B, 9–14.

Mura, T., 1987. Micromechanics of Defects in Solids. Martinus Nijhoff [revised edition].

Pak, Y.E., 1990. Crack extension force in a piezoelectric material. J. Applied Mechanics 112, 647–653.

Pak, Y.E., 1992. Circular inclusion problem in antiplane piezoelectricity. Int. J. Solids Structures 29, 2403–2419.

Parton, V.Z., 1976. Fracture mechanics of piezoelectric materials. Acta Astronaut 3, 671–683.